Coexistence of Wi-Fi 6E and 5G NR-U: Can We Do Better in the 6 GHz Bands?

Gaurang Naik, Jung-Min (Jerry) Park

Department of Electrical & Computer Engineering, Virginia Tech, Arlington, VA, USA

{gaurang, jungmin}@vt.edu

Abstract—**Regulators in the US and Europe have stepped up their efforts to open the 6 GHz bands for unlicensed access. The two unlicensed technologies likely to operate and coexist in these bands are Wi-Fi 6E and 5G New Radio Unlicensed (NR-U). The *greenfield* 6 GHz bands allow us to take a fresh look at the coexistence between Wi-Fi and 3GPP-based unlicensed technologies. In this paper, using tools from stochastic geometry, we study the impact of Multi User Orthogonal Frequency Division Multiple Access, i.e., MU OFDMA—a feature introduced in 802.11ax—on this coexistence issue. Our results reveal that by disabling the use of the legacy contention mechanism (and allowing only MU OFDMA) for uplink access in Wi-Fi 6E, the performance of both NR-U networks and uplink Wi-Fi 6E can be improved. This is indeed feasible in the 6 GHz bands, where there are no operational Wi-Fi or NR-U users. In so doing, we also highlight the importance of accurate channel sensing at the entity that schedules uplink transmissions in Wi-Fi 6E and NR-U. If the channel is incorrectly detected as idle, factors that improve the uplink performance of one technology contribute negatively to the performance of the other technology.**

Index Terms—**Wi-Fi 6E, 5G NR-U, 6 GHz coexistence.**

I. INTRODUCTION

The Federal Communications Commission (FCC) in the US recently approved spectrum sharing rules for the 6 GHz bands in its 6 GHz Report & Order [1]. Similarly, regulators in Europe are considering to allow unlicensed operations in the 6 GHz bands [2]. Arguably, Wi-Fi is the most popular unlicensed radio access technology (RAT) in use today [3]. Naturally, the IEEE 802.11 Working Group is actively working on 6 GHz rules for the upcoming IEEE 802.11ax standard of devices [4]. Wi-Fi devices certified as per the 802.11ax specifications are referred to as Wi-Fi 6 devices, while those capable of operating in the 6 GHz bands will be referred to as Wi-Fi 6E devices. Furthermore, the next generation of Wi-Fi devices—which will be based on IEEE 802.11be—are likely to be equipped with several features tailored for operations in the 6 GHz bands [5], [6]. Simultaneously, the 3rd Generation Partnership Project (3GPP) recently released the specifications for the 5G New Radio Unlicensed (NR-U) in its Release 16 [7], which includes provisions for NR-U devices to operate in the 6 GHz bands [8], [9]. Thus, spectrum sharing between Wi-Fi 6E and NR-U devices is imminent in the 6 GHz bands.

Spectrum sharing between Wi-Fi and 3GPP-based unlicensed RATs is hardly a new challenge. During the design of previous 3GPP-based unlicensed RATs—LTE Licence Assisted Access (LAA) in Rel. 13 and enhanced LAA in Rel. 14—there was a significant debate on whether these cellular-based RATs can coexist harmoniously with the millions of existing Wi-Fi networks in the 5 GHz bands [10]. After careful deliberations, to ensure that the existing Wi-Fi deployments remain unharmed, the Medium Access Control (MAC) protocol of LAA was designed to be similar to that of Wi-Fi [11]. Thus, at their core, both Wi-Fi and LAA use Listen Before Talk (LBT)-based MAC protocols for channel arbitration[1].

The 6 GHz unlicensed spectrum, on the other hand, is *greenfield* spectrum, i.e., these are bands where neither Wi-Fi nor any 3GPP-based unlicensed RATs presently operate. This has significant implications on the design of unlicensed RATs that will share the 6 GHz bands. Firstly, NR-U is no longer constrained to provide an additional degree of protection to Wi-Fi devices[2] operating in these new bands. Secondly, for the first time since the design of IEEE 802.11a, Wi-Fi 6E devices operating in the 6 GHz bands need not be backward compatible with older generations of Wi-Fi devices. Thus, the 6 GHz bands provide a rare opportunity for the design of *novel* coexistence mechanisms between unlicensed RATs [12].

In this paper, we use tools from stochastic geometry to derive an analytical model to assess the performance of Wi-Fi 6E and NR-U when they coexist. Our derived analytical model can be applied to all frequency bands in which Wi-Fi 6E and NR-U systems can operate. However, we interpret the results from our model in the context of the 6 GHz bands because these bands allow us to take measures that are otherwise not possible in the 5 GHz bands. For example, one of the critical findings in this paper is that Multi User Orthogonal Frequency Division Multiple Access (MU OFDMA)—a feature introduced to Wi-Fi in 802.11ax—can be used to improve the performance of NR-U as well as that of uplink Wi-Fi 6E transmissions. While exclusive use of MU OFDMA (i.e., disabling the LBT-based legacy contention) for uplink access is not possible in the 5 GHz bands due to the millions of already deployed Wi-Fi users, this is indeed feasible in the greenfield 6 GHz bands.

In the formulation of our analytical model, we seek an

---

[1]Note that the LBT-based MAC protocol in Wi-Fi is known as Carrier Sense Multiple Access with Collision Avoidance (CSMA/CA). Due to their functional similarities, we use the terms LBT and CSMA/CA interchangeably.

[2]In the 5 GHz bands, compared to the detection threshold used by Wi-Fi devices to detect LAA signals (-62 dBm), LAA networks used a 10 dB lower detection threshold (-72 dBm) to detect Wi-Fi signals on the air.

answer to the following question—*given that an NR-U or Wi-Fi 6E device has gained access to the medium, what is the probability that its transmission will be successful?* An NR-U or Wi-Fi 6E packet transmission is successful if the Signal-to-Interference ratio (SIR) of that packet observed at the desired receiver is greater than the threshold SIR value. In the pursuit of this answer, we identify two critical factors that significantly impact NR-U and Wi-Fi 6E performance when they coexist: (i) NR-U networks benefit when Wi-Fi 6E restricts its uplink transmissions to the schedule-based MU OFDMA mode. At the same time Wi-Fi 6E devices can themselves benefit when they use the MU OFDMA mode (as opposed to LBT-based contention) for uplink transmissions, and (ii) in both NR-U and Wi-Fi 6E networks, the entity that schedules uplink users must accurately sense the channel. If not, the very factors that improve the RAT's uplink performance contribute negatively to the success of the other RAT's ongoing transmissions.

In contrast to related research, we look at the coexistence of Wi-Fi 6E and NR-U on a per-transmission basis when one NR-U network coexists with a Wi-Fi Basic Service Set (BSS). This framework gives us the flexibility to individually study the impact of coexistence on both RATs under all possible combinations of transmission and interference directions (i.e., uplink and downlink), both operational modes of Wi-Fi 6E (i.e., LBT-based legacy contention and MU OFDMA) and the impact of transmit power control—a mandatory requirement in both uplink MU OFDMA Wi-Fi 6E and NR-U. Furthermore, we see that insights derived from this simplified scenario hold true even when multiple Wi-Fi 6E and NR-U networks coexist.

The main contributions of this paper are as follows:

- We use a stochastic geometry-based coexistence model and our in-house simulator to study the impact of MU OFDMA in Wi-Fi 6E on the coexistence performance.
- We show that two features—MU OFDMA and transmit power control—which are traditionally used to improve a given RAT's performance, also benefit Wi-Fi 6E and NR-U performance when they coexist.
- We identify two critical factors that significantly impact the performance of Wi-Fi 6E and NR-U when they coexist: (i) transmit power control used by uplink devices, and (ii) the number of scheduled uplink users.

II. RELATED WORK

There is rich literature on the coexistence between the predecessors of Wi-Fi 6/6E and NR-U, i.e., IEEE 802.11ac and LAA, respectively. These studies derive their results through experimental studies, system-level simulations, and/or analytical modeling. Chen et al. provide a comprehensive survey on the related work on LAA–Wi-Fi coexistence in [11].

In terms of stochastic geometry-based coexistence modeling, Li et al. [13] derive expressions for the medium access probability and the coverage probability for the two RATs when they coexist. Ajami et al. [14] derive expressions for similar metrics but additionally consider 802.11ax as the Wi-Fi standard, thereby considering MU OFDMA transmissions and the use of spatial re-use techniques introduced in 802.11ax.

Mbengue et al. [15] study the impact of the detection threshold on LAA and Wi-Fi performance. Wang et al. [16] and Bhorkar et al. [17] leverage stochastic geometry to evaluate coexistence between LTE-U[3] and Wi-Fi in the 5 GHz bands.

The focus of the aforementioned studies is on analyzing the performance of existing protocols rather than optimizing parameters/settings that influence coexistence, which is critical when unlicensed RATs begin to operate in a new band. Furthermore, references [13]–[17] consider LAA traffic only in the downlink, while uplink LAA traffic is ignored. Additionally, the only reference that considers MU OFDMA in IEEE 802.11ax is [14], while others look at the performance of Wi-Fi with Carrier Sense Multiple Access with Collision Avoidance (CSMA/CA). Finally, the most significant difference between related literature and this paper is the studied performance metric—we look at the coexistence problem on a per-transmission basis, which allows us to look at the NR-U–Wi-Fi 6E coexistence problem at a more granular level.

III. BACKGROUND

A. Wi-Fi 6/6E

One of the most prominent features introduced in Wi-Fi 6 to increase the MAC layer efficiency is the use of MU OFDMA [18]. Traditionally, Wi-Fi users have used CSMA/CA for channel access [19], wherein devices contend for the channel before transmitting a packet and can only transmit one at a time. Throughout this paper, we refer to CSMA/CA-based Wi-Fi transmissions as single user (SU) Wi-Fi transmissions[4]. It is well known that the performance of CSMA/CA quickly deteriorates as the number of wireless nodes increases [20].

MU OFDMA allows for the division of the channel into orthogonal frequency Resource Units (RUs), which are assigned to individual Wi-Fi stations (STAs), i.e., clients, based on their traffic demands. Downlink and uplink MU OFDMA transmissions are both initiated by the Wi-Fi 6 Access Point (AP) using a Trigger Frame (TF). As illustrated in Fig. 1, uplink MU OFDMA transmissions in Wi-Fi 6 are initiated by the AP by contending for the channel using CSMA/CA and transmitting the TF upon winning access. This TF contains resource allocation information required by the STAs to transmit in the uplink. MU OFDMA transmissions then occur at a fixed interval of 16 μsec after receiving the TF.

In downlink MU OFDMA, the AP transmits a single frame that contains packets addressed to all the assigned STAs. Upon reception, this packet is decoded by the relevant STAs. On the other hand, STAs *scheduled* by the AP for uplink start transmitting on their designated RUs. Since the channel availability can be different at the AP and the scheduled STA(s), each scheduled STA senses the medium once again before transmitting. If the channel is busy at the STA(s), the

---

[3]LTE-U is an unlicensed flavor of LTE developed by an industry forum that uses adaptive duty-cycling instead of LBT for coexistence.

[4]Note that beamforming-based MU transmissions also operate using CSMA/CA-based legacy channel contention. However, accounting for such transmissions requires consideration of directional sensing [9], the rigorous analysis of which is beyond the scope of this paper.
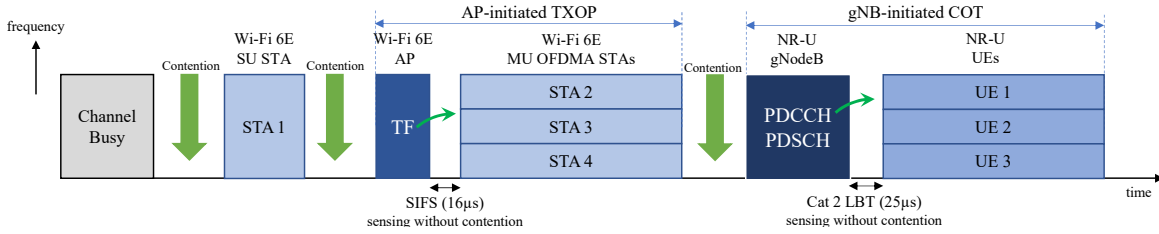
Fig. 1: An illustration of SU and MU OFDMA transmissions in Wi-Fi 6E and NR-U transmissions. Packet ACKs are not shown.

STA(s) will refrain from transmitting. However, if the channel is idle, the STA(s) do not perform exponential back-off and proceed with their transmissions. The exchange of TF, uplink MU OFDMA packets and the acknowledgment (ACK) occurs in a single transmit opportunity (TXOP), which is initiated by the AP when it gains access to the channel during the transmission of the TF. It is worthwhile to note that uplink MU OFDMA transmissions in Wi-Fi 6 use a *hybrid* LBT (at the AP) and schedule-based (at the STAs) transmission approach.

In the uplink, the number of concurrently transmitting STAs can be more than one. Although these transmissions occur on orthogonal RUs, if the received signal strength on these RUs at the AP varies considerably, adjacent-RU interference can impair the reception of signals sent by far-away STAs. Therefore, the 802.11ax standard makes it mandatory for uplink MU OFDMA users to use transmit power control [4]. Transmit power control ensures that the received signal strengths across different RUs have smaller variations, thereby facilitating the successful reception of packets on all RUs.

B. 5G NR-U

The specifications for 5G NR-U were recently released by the 3GPP in its Release 16 [7]. The channel access mechanism for data traffic in NR-U is based on Category 4 LBT—one of the four LBT categories defined by the 3GPP [7], [21], which is functionally similar to Wi-Fi's CSMA/CA protocol. To ensure fair channel access with Wi-Fi devices, the MAC protocol parameters chosen in NR-U are the same as those used by Wi-Fi [8]. Like the Wi-Fi 6/6E AP, the NR-U gNB transmits in the downlink by contending for the channel using LBT. Uplink NR-U transmissions, on the other hand, use the hybrid LBT and scheduled approach (similar to Wi-Fi 6/6E MU OFDMA, see Fig. 1), whereby the gNB first contends for the medium and, if the channel is idle, schedules a fixed number of NR-U user equipments (UEs) for uplink transmissions. The resource allocation information for uplink transmissions is contained in the Physical Downlink Control Channel (PDCCH), which is the downlink logical control channel in NR (the downlink logical channel for data transmissions is referred to as the Physical Downlink Shared Channel, PDSCH). The assigned UEs can then transmit using category 2 LBT, wherein the UEs sense the medium for a fixed interval of 25 μsec, but do not perform random back-off. The entire exchange of PDSCH/PDCCH and the uplink transmissions is completed within the gNB-initiated Channel Occupancy Time (COT). Furthermore, like MU OFDMA STAs, UEs transmitting in the uplink use transmit power control.

IV. SYSTEM MODEL

A. Notations

An italicized variable t denotes an instance of a random variable T. The probability density function (pdf), cumulative distribution function (cdf) and moment generating function (mgf) of T are denoted as $f_T(.)$, $\mathbb{F}_T(.)$ and $\Phi_T(.)$, respectively. $\mathcal{L}^{-1}(.)$ is the Laplace inverse operator and $\mathrm{Re}\{.\}$ denotes the real part of a complex quantity. Further, $|.|$ indicates the cardinality of a set. A parameter or random variable written as T^{YZ} or T_{YZ} indicates that the parameter/random variable is computed for a scenario where RAT Y device(s) is/are transmitting and RAT Z devices act as potential interferers.

B. Setup

We consider a scenario where a Wi-Fi 6E BSS operates in the close proximity of an NR-U network. The two networks operate on the same channel, thereby sharing the channel, and potentially interfering with each other. The Wi-Fi 6E BSS comprises of one AP and M_W STAs, while the NR-U network comprises of one gNB and M_N UEs. The devices are randomly and uniformly located inside a circular region $\mathcal{C}(o, \mathrm{R})$ of radius R and centered at the origin, o, as shown in Fig. 2. In practical networks, $\mathcal{C}(o, \mathrm{R})$ can be thought of as the smallest circular region that encloses all Wi-Fi 6E and NR-U devices associated with the Wi-Fi 6E AP and the NR-U gNB, respectively. The locations of Wi-Fi 6E and NR-U devices are modeled as two independent Binomial Point Processes (BPPs), Ψ_W and Ψ_N, respectively, such that $|\Psi_W| = M_W + 1$ and $|\Psi_N| = M_N + 1$. The BPPs corresponding to the active Wi-Fi 6E and NR-U transmitters are denoted as Ψ_W^T and Ψ_N^T, respectively, where $\Psi_W^T \subset \Psi_W$ and $\Psi_N^T \subset \Psi_N$. Let $|\Psi_W^T| = M_W^T$ and $|\Psi_N^T| = M_N^T$. The list of notations used in this paper are outlined in Table I.
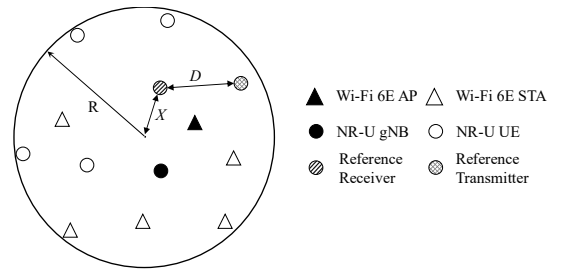

Fig. 2: System model: uniform distribution within $\mathcal{C}(o, \mathrm{R})$.

C. Assumptions

We make the following assumptions in our analysis.

TABLE I: Summary of notations used in the paper.

Notation	Definition
$\mathcal{C}(o,\mathrm{R})$	Circular region where all devices are located, centered at o and of radius R
η	Path loss exponent
g	Constant path loss factor
K	Fading coefficient
Ψ_W/Ψ_N	BPP that defines Wi-Fi 6E/NR-U device locations
Ψ_W^T/Ψ_N^T	BPP for the locations of active Wi-Fi 6E/NR-U transmitters
M_W/M_N	Total number of Wi-Fi 6E STAs/NR-U UEs
M_W^T/M_N^T	Number of active Wi-Fi 6E/NR-U transmitters
P_{AP}/P_{STA}	Transmit power of Wi-Fi 6E AP/STA
P_{gNB}/P_{UE}	Transmit power of NR-U gNB/UE
β_{YZ}	Threshold used by RAT Z devices to detect RAT Y transmissions
γ_Y	Min. SIR required to decode RAT Y transmissions
ϵ_Y/ϵ_Z	Fractional power control parameter used by RAT Y/Z
X	R.V. denoting the distance of a point from o
D	R.V. denoting the distance between two arbitrary points in $\mathcal{C}(o,\mathrm{R})$ given one of the points is at $X=x$
Q_{YZ}	R.V. denoting the number of hidden RAT Z devices during ongoing RAT Y transmissions
Q_{YZ}^{max}	Max. no. of hidden RAT Z devices when RAT Y transmits
Q_Z^{sch}	Number of scheduled uplink users, i.e., STAs for MU OFDMA uplink Wi-Fi 6E and UEs for uplink NR-U
p_H^{YZ}	Prob. that a given device of RAT Z is hidden to ongoing RAT Y transmission(s)
$p_{H,x}^{YZ}$	Prob. that a given device of RAT Z, located at X = x, is hidden to ongoing RAT Y transmission(s)
p_S^Y	Prob. that a given RAT Y transmission is successful
$p_{S,q}^Y$	Prob. that a given RAT Y transmission is successful given q fixed RAT Z interferers

1) Path loss & fading: We use the decaying path loss model with exponent η, where the received power (P_R) at a distance d from the transmitter is $P_R = P_T g K d^{-\eta}$. Here, P_T is the transmit power, g is a constant, and K is the fading coefficient. The channel is assumed to undergo Rayleigh fading [13], [14].

2) Full buffer traffic: We assume that all nodes in the network always have a packet to transmit. Despite this assumption, MU OFDMA STAs and NR-U UEs transmit only when scheduled by the AP/gNB.

3) SU Wi-Fi 6E transmissions: We assume that if one of the M_W SU STAs in the BSS transmits, the other STAs sense the signal and back-off. This is a fair assumption because Wi-Fi devices use preamble detection (with a threshold of -82dBm) and virtual carrier sensing [19] to detect other Wi-Fi signals (see Fig. 3(c)). We relax this assumption in our simulations.

4) Independence of the hidden node probability: We assume that the probability of a node being hidden to ongoing transmission(s) is independent of its location in $\mathcal{C}(o,\mathrm{R})$. This is not true in general [22]. In fact, Sec. V-A computes the hidden node probability by averaging over all possible node locations. However, we see in Sec. VI that this assumption has a very small impact on the computed metrics.

5) Interference-limited: We assume that Wi-Fi 6E and NR-U are interference-limited—a widely used assumption [23].

D. Distributions & Power Computation

For performance analysis, we look at the received signal strength at a device that is arbitrarily located inside $\mathcal{C}(o,\mathrm{R})$. The distance of this point (location) from the origin, o, is denoted by a random variable X, whose pdf is given by

Eq. (1) [24]. Given that the location of this *reference* receiver is $X = x$, the distance between this receiver and an arbitrary *reference* transmitter in $\mathcal{C}(o,\mathrm{R})$ is denoted by a random variable D (see Fig. 2), whose pdf is given by Eq. (2) [24].

$$f_X(x) = \frac{2x}{\mathrm{R}^2}, \qquad 0 \le x \le \mathrm{R}. \tag{1}$$

$$f_D(d) = \begin{cases} \frac{2d}{\mathrm{R}^2}, & 0 \le d \le \mathrm{R} - x, \\ \frac{2d}{\pi\mathrm{R}^2}\cos^{-1}\left(\frac{d^2+x^2-\mathrm{R}^2}{2xd}\right), & \mathrm{R} - x \le d \le \mathrm{R} + x. \end{cases} \tag{2}$$

The transmit powers of the AP, STAs, gNB and UEs are denoted as P_{AP}, P_{STA}, P_{gNB} and P_{UE}, respectively. MU OFDMA Wi-Fi 6E STAs and NR-U UEs use fractional transmit power control with parameter ϵ for uplink transmissions [25]. The transmit power of a generic device located at a distance d_1 from its intended receiver is given by Eq. (3), where $P_Y \in \{P_{AP}, P_{STA}\}$ for Wi-Fi 6E devices and $P_Y \in \{P_{gNB}, P_{UE}\}$ for NR-U devices. If the transmitting device is a Wi-Fi 6E AP, SU STA, or NR-U gNB, $\epsilon = 0$, i.e., no power control is used, while $\epsilon \ge 0$ for MU OFDMA STAs and NR-U UEs. Using the path loss model described in assumption 1, the received power from this transmission at an arbitrary device located at a distance d_2 from the transmitter is then given by Eq. (4).

$$P_T(d_1) = P_Y d_1^{\eta\epsilon}. \tag{3}$$

$$\begin{aligned} P_R(d_1, d_2) &= P_T(d_1)gK d_2^{-\eta} \\ &= g P_Y K d_1^{\eta\epsilon} d_2^{-\eta}. \end{aligned} \tag{4}$$

V. PERFORMANCE ANALYSIS

In this section, we derive an expression for the success probability of a given (Wi-Fi 6E/NR-U) RAT's transmissions given that these devices have gained access to the channel. The RAT that gains access to the channel first is referred to as "Y", while the potentially interfering RAT is referred to as "Z". For example, when Wi-Fi 6E devices transmit, Y=W (i.e., Wi-Fi) and Z=N (i.e., NR-U), and vice-versa.

The two RATs coexist by sensing each other and ceasing their transmissions when the channel is detected as busy. If the strength of the signal transmitted by the RAT Y device(s) at a RAT Z device is lower than the detection threshold[5], β_{YZ}, the devices are *hidden* to each other. Thereafter, the hidden RAT Z device can transmit and interfere at the RAT Y receiver.

Since we focus on the investigation of inter-RAT coexistence, we ignore intra-RAT hidden nodes, i.e., hidden Wi-Fi (or NR-U) nodes when other Wi-Fi (or NR-U) devices transmit. Note that in our system model, intra-RAT interference can only originate from SU Wi-Fi 6E STAs transmitting in the uplink. This is because uplink MU OFDMA and NR-U transmissions occur only when scheduled by the AP/gNB. Further, our implicit assumption in this section is that NR-U and Wi-Fi 6E devices contend on a 20 MHz channel. However,

---

[5]The detection threshold is collectively defined by "Y" and "Z". In the 5 GHz bands, $\beta_{WW}=-82$dBm, $\beta_{NW}=-62$dBm, and $\beta_{WN}=\beta_{NN}=-72$dBm for a 20 MHz channel.

the analysis easily extends to wider channel bandwidths by selecting the appropriate detection threshold in Eq. (5) and considering only the overlapping interference in Eq. (18).

A. The Hidden Node Probability

An arbitrary RAT Z device is hidden to RAT Y transmissions if the total power received from these transmissions at the RAT Z device is less than the detection threshold, β_{YZ}. Given that the reference RAT Z device is located at $X = x$, the probability that it is hidden to ongoing RAT Y transmissions is denoted as $p_{\text{H},x}^{\text{YZ}}$ and given by Eq. (5), where D_{bi} denotes the RAT Y transmitter's distance from its intended receiver and D_i denotes the distance between the RAT Y transmitter and the reference RAT Z receiver. The pdf of D_{bi} and D_i is given by Eq. (2). Further, $\beta_{\text{YZ}}' = \frac{\beta_{\text{YZ}}}{g P_{\text{Y}}}$, and T_x is a dummy random variable defined as: $T_x = \sum_{i=1}^{\text{M}_{\text{Y}}^{\text{T}}} K_i D_i^{-\eta} D_{bi}^{\eta_{\epsilon_{\text{Y}}}}$.

$$
\begin{aligned}
p_{\text{H},x}^{\text{YZ}} &= \mathbb{P}\left(\sum_{i \in \Psi_{\text{Y}}^{\text{T}}} P_{\text{T}}(D_{bi}) g K_i D_i^{-\eta} < \beta_{\text{YZ}}\right) \\
&= \mathbb{P}\left(\sum_{i=1}^{\text{M}_{\text{Y}}^{\text{T}}} K_i D_i^{-\eta} D_{bi}^{\eta_{\epsilon_{\text{Y}}}} < \beta_{\text{YZ}}'\right) \\
&= \mathbb{P}\left(T_x < \beta_{\text{YZ}}'\right) = \mathbb{F}_{T_x}\left(\beta_{\text{YZ}}'\right).
\end{aligned}
\tag{5}
$$

Averaging over all possible locations of the reference RAT Z device, we get the average hidden node probability in Eq. (6).

$$
p_{\text{H}}^{\text{YZ}} = \mathbb{E}_X\left(p_{\text{H},x}^{\text{YZ}}\right) = \int_0^{\text{R}} \frac{2x}{\text{R}^2}\, p_{\text{H},x}^{\text{YZ}}\, \mathrm{d}x.
\tag{6}
$$

To compute the distribution of T_x, we first derive an expression for the mgf of T_x, i.e., $\Phi_{T_x}(s)$. The cdf of T_x can then be obtained as,

$$
\mathbb{F}_{T_x}(t) = \mathcal{L}^{-1}\left[\frac{\Phi_{T_x}(s)}{s}\right].
\tag{7}
$$

Sources of randomness in T_x are the fading coefficients K_i and the distances — D_i and D_{bi}. To compute the mgf of T_x, we need the joint pdf $f_{K_i, D_{bi}, D_i}(k, d_{bi}, d_i)$. We assume that K_i, D_{bi} and D_i are independent of each other. Therefore, $f_{K_i, D_{bi}, D_i}(k, d_{bi}, d_i) = f_K(k) \cdot f_D(d_{bi}) \cdot f_D(d_i)$. Further, due to the Rayleigh fading assumption, K is an exponential random variable. We assume that the mean of K is 1. Thus, the pdf of K is given by $f_K(k) = e^{-k}, 0 \leq k < \infty$ [13]. The mgf of T_x can be obtained as shown in Eq. (8).

$$
\begin{aligned}
\Phi_{T_x}(s) &= \mathbb{E}_{K_i, D_{bi}, D_i}\{\exp(-s T_x)\} \\
&= \mathbb{E}_{K_i, D_{bi}, D_i}\left\{\exp\left(-s \sum_{i=1}^{\text{M}_{\text{Y}}^{\text{T}}} k_i d_i^{-\eta} d_{bi}^{\eta_{\epsilon_{\text{Y}}}}\right)\right\} \\
&= \left(\mathbb{E}_{K_i, D_{bi}, D_i}\left\{\exp\left(-s k_i d_i^{-\eta} d_{bi}^{\eta_{\epsilon_{\text{Y}}}}\right)\right\}\right)^{\text{M}_{\text{Y}}^{\text{T}}} \\
&= \left(\int_{D_{bi}} \int_{D_i} f_D(d_{bi}) f_D(d_i) \left(\frac{1}{s d_i^{-\eta} d_{bi}^{\eta_{\epsilon_{\text{Y}}}} + 1}\right) \mathrm{d}d_i\, \mathrm{d}d_{bi}\right)^{\text{M}_{\text{Y}}^{\text{T}}}.
\end{aligned}
\tag{8}
$$

The pdf of D from Eq. (2) can be substituted in Eq. (8) to obtain an expression for $\Phi_{T_x}(s)$. The resulting expression is a summation of four double integrals (since the pdf of D is defined over two intervals, i.e., 0 to $\text{R}-x$, and $\text{R}-x$ to $\text{R}+x$). Due to the presence of the $\cos^{-1}$ term in Eq. (2), however, Eq. (8) does not have a closed-form expression. Therefore, Eq. (8) and all subsequent integrals involving $\Phi_{T_x}(s)$ require numerical solution of integrals.

Eq. (8) can be substituted in Eq. (7) and evaluated at β_{YZ}' to obtain $p_{\text{H},x}^{\text{YZ}}$ (see Eq. (5)). Then, p_{H}^{YZ} can be computed using Eq. (6). In order to get $\mathbb{F}_{T_x}(\beta_{\text{YZ}}')$, however, a Laplace inverse operation is required, which must be computed numerically. We use the approach provided in [24] as shown in Eq. (9).

$$
\mathbb{F}_{T_x}(\beta_{\text{YZ}}') = \frac{2^{-H} \exp(A/2)}{\beta_{\text{YZ}}'} \sum_{h=0}^{H} \binom{H}{h} \sum_{c=0}^{C+h} \frac{(-1)^c}{E_c} \text{Re}\left\{\frac{\Phi_{T_x}(s)}{s}\right\},
\tag{9}
$$

where the parameters A, H and C are chosen as $\zeta \ln(A), 1.243\zeta - 1$ and 1.467ζ, respectively, to achieve an estimation accuracy of $10^{-\zeta}$ (we use $\zeta = 8$). Further, $s = \frac{(A + \mathbf{i} 2\pi c)}{2\beta_{\text{YZ}}'}$, and the parameter $E_c = 2$, if $c = 0$, and $E_c = 1$, otherwise.

B. Probability Mass Function for the Number of Interferers

We now estimate the number of RAT Z devices that are hidden to RAT Y transmission(s). From assumption 4, we have the same hidden node probability, p_{H}^{YZ}, for all RAT Z devices. Let Q_{YZ} and $Q_{\text{YZ}}^{\text{max}}$ denote the actual and maximum number of RAT Z devices hidden to RAT Y transmissions, respectively.

First, consider the case where Wi-Fi 6E uses MU OFDMA in the uplink. In this scenario, the operations of Wi-Fi 6E and NR-U are similar. The AP/NR-U transmits in the downlink by using LBT to contend for the medium. Upon winning access, the AP/gNB transmits its packet. This implies that if RAT Z has traffic in the downlink, the only possible interferer is the AP/gNB, which interferes with RAT Y transmission(s) if it is hidden. Thus, the number of interferers can be either 0 or 1, i.e., $Q_{\text{YZ}}^{\text{max}} = 1$ for RAT Z downlink interference. The corresponding probabilities are given in Eq. (10) and Eq. (11).

For uplink transmissions, the AP/gNB first senses the channel and, if idle, schedules the STA(s)/UE(s) (see Fig. 1). This is followed by sensing at the STA(s)/UE(s). If the channel is idle at the STA(s)/UE(s) as well, an uplink transmission is initiated. If the AP/gNB is not hidden, it will not schedule uplink transmissions. However, if the AP/gNB is hidden it can schedule users in the uplink and any of these scheduled users can potentially be hidden to the ongoing RAT Y transmission(s). Thus, if RAT Z has traffic in the uplink, the maximum number of interferers is equal to the number of scheduled uplink devices (which we denote as $Q_{\text{Z}}^{\text{sch}}$), i.e., $Q_{\text{YZ}}^{\text{max}} = Q_{\text{Z}}^{\text{sch}}$. The number of uplink interferers is 0 in two cases (see Eq. (12)), (i) the AP/gNB can sense ongoing RAT Y transmissions, or (ii) the AP/gNB is hidden but all of the $Q_{\text{YZ}}^{\text{max}}(= Q_{\text{Z}}^{\text{sch}})$ STAs/UEs can sense the ongoing RAT Y transmissions. On the other hand, the number of interferers is j, where $j > 0$, if (i) the AP/gNB is hidden, *and* (ii) j of the $Q_{\text{Z}}^{\text{sch}}$ scheduled uplink users are hidden. The resulting probability is given in Eq. (13).

Now consider the case where Wi-Fi 6E users operate in the SU mode using LBT-based legacy contention. In this scenario, since STAs need not be scheduled by the AP to transmit, any of the hidden STA(s) can initiate a transmission and act as a potential interferer. Using assumptions 2 and 3, the number of interferers is zero if none of the M_W Wi-Fi 6E STAs are hidden. On the other hand, the number of interferers is one if at least one of the M_W STAs is hidden to NR-U transmissions. The corresponding probabilities are given in Eq. (14) and (15).

TABLE II: Probability mass function of Q_{YZ}, $\mathbb{P}(Q_{YZ} = q)$.

Case	Value (q)	Q_{YZ}^{max}	Probability, $\mathbb{P}(Q_{YZ} = q)$	
Down-	0	1	$(1 - p_H^{YZ})^{Q_{YZ}^{max}} = 1 - p_H^{YZ}$	(10)
link	1		$1 - (1 - p_H^{YZ})^{Q_{YZ}^{max}} = p_H^{YZ}$	(11)
Up-	0	Q_Z^{sch}	$1 - p_H^{YZ} + p_H^{YZ}(1 - p_H^{YZ})^{Q_{YZ}^{max}}$	(12)
link	$j > 0$		$p_H^{YZ} \binom{Q_{YZ}^{max}}{j} \left(p_H^{YZ}\right)^j \left(1 - p_H^{YZ}\right)^{Q_{YZ}^{max} - j}$	(13)
SU	0	1	$(1 - p_H^{YZ})^{M_W}$	(14)
Wi-Fi	1		$1 - (1 - p_H^{YZ})^{M_W}$	(15)

C. Success Probability

Finally, we compute the success probability of a given RAT Y transmission, which is denoted as p_S^Y. First, we let the number of RAT Z interferers be fixed to q and compute the resulting RAT Y success probability, denoted by $p_{S,q}^Y$. The probability p_S^Y can then be computed as given by Eq. (16).

$$p_S^Y = \sum_{q=0}^{Q_{YZ}^{max}} \mathbb{P}(Q_{YZ} = q) \times p_{S,q}^Y, \tag{16}$$

In Eq. (16), $\mathbb{P}(Q_{YZ} = q)$ is computed using Table II. From assumption 5, we have $p_{S,0}^Y = 1$. Given that the number of RAT Z interferers is fixed to q, the probability that the RAT Y transmission is successful can be computed as follows.

$$p_{S,q}^Y = \mathbb{E}_X \left\{ p_{S,q,x}^Y \right\} = \int_0^R f_X(x) \, p_{S,q,x}^Y \, dx, \tag{17}$$

where $p_{S,q,x}^Y$ denotes the probability that a given transmission of RAT Y is successful given that the number of interferers is fixed to $Q_{YZ} = q$ and the RAT Y receiver is located at $X = x$. The expression for $p_{S,q,x}^Y$ can be derived as shown in Eq. (18).

$$
\begin{aligned}
p_{S,q,x}^Y &= \mathbb{P}\left(\frac{P_Y g K_b D_b^{\eta(\epsilon_Y - 1)}}{\sum_{l=1}^q P_Z g K_l D_{(2l-1)}^{\eta\epsilon_Z} D_{(2l)}^{-\eta}} \geq \gamma_Y \right) \\
&= \mathbb{E}\left\{ \mathbb{P}\left(K_b \geq \gamma_Y' d_b^{\eta(1-\epsilon_Y)} \left[\sum_{l=1}^q k_l d_{(2l-1)}^{\eta\epsilon_Z} d_{(2l)}^{-\eta} \right] \right) \right\} \\
&\stackrel{(a)}{=} \mathbb{E}\left\{ \exp\left(-\gamma_Y' d_b^{\eta(1-\epsilon_Y)} \left[\sum_{l=1}^q k_l d_{(2l-1)}^{\eta\epsilon_Z} d_{(2l)}^{-\eta} \right] \right) \right\} \\
&\stackrel{(b)}{=} \mathbb{E}\left\{ \prod_{l=1}^q \left(\frac{1}{1 + \gamma_Y' d_b^{\eta(1-\epsilon_Y)} d_{(2l-1)}^{\eta\epsilon_Z} d_{(2l)}^{-\eta}} \right) \right\},
\end{aligned}
\tag{18}
$$

where γ_Y is the minimum SIR required to decode the RAT Y signal at the receiver, D_b is the distance between the RAT Y transmitter and its desired receiver, and $\gamma_Y' = \frac{P_Z \gamma_Y}{P_Y}$. Note that

the denominator of Eq. (18) contains $D_{(2l-1)}$ and $D_{(2l)}$, which denote the distance between the interferer and its desired receiver, and the distance between the interferer and RAT Y receiver, respectively. However, since these two represent the same distance for the RAT Y transmitter, there is only one such term in the numerator (i.e., D_b). Further, (a) follows from the complementary cdf of an exponential random variable, while (b) is obtained by taking expectation over all K_l, and given that $\int_0^\infty e^{-k} e^{-tk} \, dk = \frac{1}{1+t}$ for $t \geq 0$. Taking expectations over D_b, $D_{(2l-1)}$, $D_{(2l)}$ and finally over X (see Eq. (17)), we get the expression for $p_{S,q}^Y$ as shown in Eq. (19).

VI. SIMULATION & NUMERICAL RESULTS

The numerical results presented in this section are generated using Matlab's numerical integration functions for up to four integrals. When the number of integrals is more than four, we use Monte Carlo integration with uniform sampling within the integration region. Simulation results have been generated using our Matlab-based in-house NR-U and Wi-Fi 6E simulator. The simulator is modular, configurable, and models the MAC layers of Wi-Fi 6E (CSMA/CA-based contention and MU OFDMA) and NR-U (the LBT protocol), along with packet collisions. The PHY layer is abstracted such that all packets received above the threshold SIR are forwarded to the MAC layer, while those below the threshold SIR are dropped.

Unless explicitly stated otherwise, lines with error bars indicate simulation results, where the error bars show the 95% confidence interval. Throughout this section, we refer to Wi-Fi 6E devices simply as Wi-Fi devices. Wi-Fi and NR-U parameters used in this section are outlined in Table III. We choose the parameters $g = 10^{-4}$ and $\eta = 4$ in Eq. (4) such that the path loss (without fading) predicted by Eq. (4) matches with the predictions of the WINNER+ A1 non-line-of-sight model [26], which emulates an office-like indoor setting.

TABLE III: Simulation parameters

Parameter	Value	Parameter	Value
R	4 to 25	γ_W, γ_N	4.3 dB
g	10^{-4}	η	4
P_{AP}, P_{gNB}	23 dBm	P_{STA}, P_{UE}	14 dBm [27]
M_W, M_N	1 to 9	M_W^T, M_N^T	1,3,9
ϵ_W, ϵ_N	0, 0.2, 0.5, 1 (uplink) 0 (downlink)	Q_W^{sch}, Q_N^{sch}	1 to 5
Pkt. size	1000 Bytes	PHY rate	24 Mbps

A. Validation of Analysis

In Fig. 3(a) and Fig. 3(b), we report results for a scenario where Wi-Fi STAs transmitting in the uplink MU OFDMA mode interfere with ongoing uplink NR-U transmissions. Fig. 3(a) shows that despite our assumption that the hidden node probability p_H^{NW} is independent of the location of the RAT Z (Wi-Fi, in this case) interferer, i.e., assumption 4, there is a close match in the analytical and simulated values for $\mathbb{P}(Q_{NW} = q)$. Similarly, Fig. 3(b) shows that for a fixed number of interferers, the success probability derived in Eq. (19) matches exactly with the simulation results. Fig. 3(c) shows that p_H^{WW}, i.e., the probability that Wi-Fi devices are

$$p_{S,q}^{Y} = \int_{X}\int_{D_b}\underbrace{\int_{D_1}\int_{D_2}\cdots\int_{D_{(2q)}}}_{2\times q \text{ integrals}}\left\{f_X(x)f_D(d_b)\underbrace{f_D(d_1)f_D(d_2)\cdots f_D(d_{(2q)})}_{2\times q \text{ terms}}\prod_{l=1}^{q}\left(\frac{1}{1+\gamma'_Y d_b^{\eta(1-\epsilon_Y)}d_{(2l-1)}^{\eta\epsilon_Z}d_{(2l)}^{-\eta}}\right)\right\}\mathrm{d}d_{(2q)}\cdots\mathrm{d}d_1\,\mathrm{d}d_b\,\mathrm{d}x$$

$$(19)$$
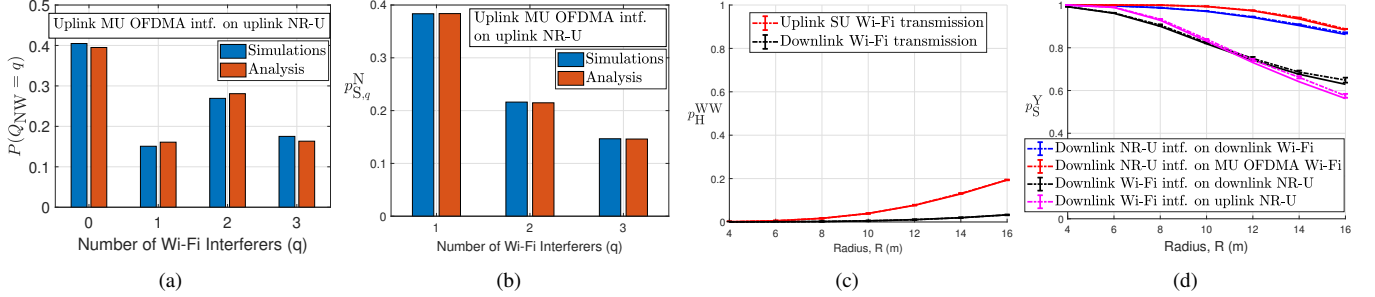
Fig. 3: Validation of analysis, $\epsilon_W=\epsilon_N=0$ for all plots, (a) No. of interferers when MU OFDMA Wi-Fi STAs interfere with NR-U uplink, $M_N^T=1$, $Q_W^{sch} = 3$, $\beta_{NW}=-62$dBm, (b) Success prob. when no. of interferers is fixed, $M_N^T=1$, $Q_W^{sch} = 3$, (c) Hidden node prob. for Wi-Fi devices when other Wi-Fi devices transmit, $\beta_{WW}=-82$ dBm, (d) Impact of 5 GHz detection thresholds, Wi-Fi 6E in the MU OFDMA mode, $\beta_{NW}=-62$dBm, and $\beta_{WN}=-72$dBm, $M_W^T=M_N^T=3$ for uplink RAT Y transmissions.

hidden to other Wi-Fi transmissions is very small (due to $\beta_{WW}=-82$dBm), thereby justifying assumption 3. Finally, Fig. 3(d) and Fig. 4 through Fig. 6 show that the derived expressions for p_S^Y for various cases agree closely with the simulation results, thereby validating our analysis.
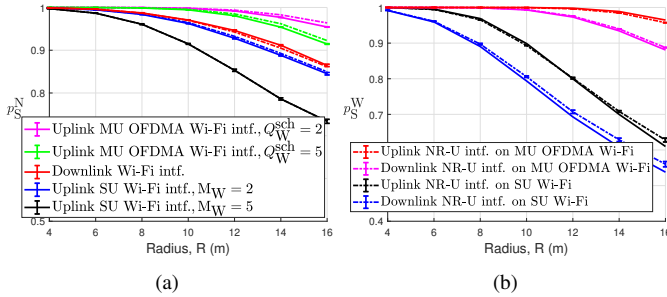

Fig. 4: Legacy contention (SU) vs MU OFDMA for Wi-Fi, $\epsilon_W=\epsilon_N=0$, (a) Impact of Wi-Fi intf. on NR-U downlink, (b) Impact of NR-U on Wi-Fi uplink, $M_W^T=3$ for MU OFDMA, $Q_N^{sch}=3$ for uplink intf.

B. Unfairness of 5 GHz Detection Thresholds

Fig. 3(d) shows the performance of NR-U and Wi-Fi for the 5 GHz detection thresholds. We see that in the presence of downlink Wi-Fi (or NR-U) interference, as the radius, R, increases, the success probability of both uplink and downlink NR-U (or Wi-Fi) drops. This drop comes from the increase in the hidden node probability p_H^{NW} (or p_H^{WN}) as R increases. However, due to the different thresholds used by Wi-Fi and NR-U to detect each other in the 5 GHz bands ($\beta_{NW}=-62$dBm and $\beta_{WN}=-72$dBm), when all other Wi-Fi and NR-U operational aspects are identical (for e.g. when the number of scheduled RAT Y users in the uplink is the same, $M_W^T=M_N^T=3$, or when RAT Y transmits in the downlink) *for most values of R, the success probability of NR-U is consistently 20-30% lower than that of Wi-Fi*. Although this unfairness issue is widely known in the literature [28], certain contributions (such as [29]) argue

for maintaining the *status quo* for channel access parameters in the 6 GHz bands. However, Fig. 3(d) reiterates the need to use the same detection threshold across all coexisting technologies in the 6 GHz bands. Hereafter, unless explicitly stated otherwise, we use $\beta_{WN}=\beta_{NW}=-72$dBm.

C. Benefits of MU OFDMA over LBT-based contention

1) Performance for a given set of detection thresholds: Fig. 4(a) shows the impact of Wi-Fi interference on NR-U downlink. The interfering RAT (Wi-Fi) can operate in three settings: (i) downlink[6], (ii) uplink SU, and (iii) uplink MU OFDMA. For a fair comparison between the latter two cases, power control is disabled for uplink MU OFDMA STAs (since $\epsilon_W=0$ for SU STAs), and we present results on the impact of uplink Wi-Fi interference (in the SU and MU OFDMA cases) when the number of *potential* interferers is the same for the two cases. Thus, if the *hidden* Wi-Fi AP schedules 2 (or 5) STAs, we compare the resulting impact with the scenario where there are 2 (or 5) SU STAs in the BSS.

Fig. 4(a) shows that even if there are only two SU Wi-Fi STAs in the BSS, their impact on NR-U is worse than downlink Wi-Fi interference. This is despite the 9 dB higher power used by the AP (see Table III). If there are more than two STAs in the BSS (e.g., 5 STAs), we see that uplink SU STAs have a far worse impact on NR-U performance than either downlink or uplink MU OFDMA interference. Furthermore, compared to uplink SU STAs, for the same number of potential interferers, uplink MU OFDMA STAs have a significantly lower impact on NR-U performance. This is because: for a MU OFDMA STA to interfere at the UE, the transmitting gNB must be hidden to the AP *as well as* at the MU OFDMA STA. On the other hand, SU STAs transmit in a distributed fashion. If *any* of the SU STAs in

---

[6]Note that as far as Wi-Fi downlink is concerned, there is no difference between downlink MU OFDMA and downlink SU transmissions.

the BSS is hidden, it senses the channel idle and can initiate a transmission, thereby interfering at the UE. Thus, the added requirement of sensing at the AP (in addition to the STAs) for initiating uplink transmissions in the MU OFDMA mode offers better protection to NR-U transmissions.

Although Fig. 4(a) shows the impact of Wi-Fi interference on downlink NR-U, we have verified that the same phenomenon is true for uplink NR-U transmissions—for the same number of potential interferers, interference from uplink SU STAs is significantly worse than interference from uplink MU OFDMA STAs. For the parameters chosen in Table III, the only scenario where downlink Wi-Fi has a worse impact on NR-U transmissions (than uplink SU Wi-Fi) is when $M_W=1$, i.e., there is only one potential SU interferer in the BSS.

Fig. 4(b) further reveals that MU OFDMA transmissions in Wi-Fi are not only beneficial for NR-U performance (when Wi-Fi is the interfering RAT) but also for the success of uplink Wi-Fi transmissions. Specifically, we see that as long as the AP schedules more than one MU OFDMA STA ($M_W^T=3$ in Fig. 4(b)), the success probability of resulting uplink Wi-Fi transmissions is considerably higher than uplink SU transmissions. This improvement stems from the increase in the number simultaneously active transmitters (3 in Fig. 4(b)) as we will discuss in Sec. VI-D1. Note that if only one MU OFDMA STA is scheduled (i.e., if $M_W^T=1$), the resulting Wi-Fi success probability is the same as in the uplink SU scenario. However, since MU OFDMA was introduced in Wi-Fi for improving the Wi-Fi MAC layer efficiency, the AP has a strong incentive to always schedule more than one STA in the uplink.
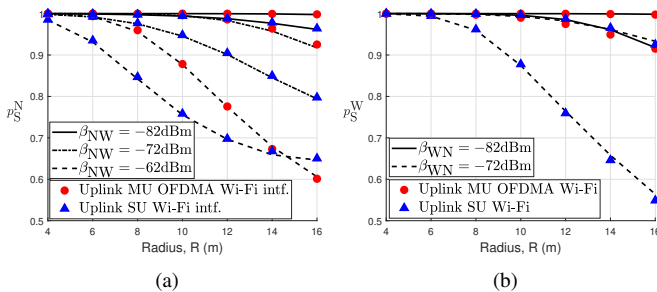

Fig. 5: Relative impact of different detection thresholds, markers indicate simulation results, (a) Impact of uplink Wi-Fi intf. on NR-U downlink, ϵ_W=0.2, Q_W^{sch}=3, (b) Impact of uplink NR-U intf. on Wi-Fi uplink, ϵ_W=ϵ_N=0.2, M_W^T=1, Q_N^{sch}=3.

2) Relative impact of the detection threshold: Fig. 5(a) shows the impact of uplink Wi-Fi interference on the success probability of downlink NR-U transmissions. Unsurprisingly, we see that as β_{NW} is lowered, the hidden node probability, p_{NW}^H, reduces and consequently, the success probability of NR-U, p_S^N, increases. Similarly, we see in Fig. 5(b), which shows the impact of uplink NR-U interference on uplink Wi-Fi performance, that a lower β_{WN} increases the success probability of both SU and MU OFDMA uplink Wi-Fi transmissions, p_S^W.

The key observation in Fig. 5(a), however, is that the performance of NR-U remains practically unaffected for small (and more practical) values of the radius, R, if the detection threshold is raised by 10dB (from $\beta_{NW} = -82$dBm to $\beta_{NW} = $

-72dBm) while switching Wi-Fi interference from the SU mode to the MU OFDMA mode. This is also true when NR-U UEs transmit in the uplink (not shown). Similarly, Fig. 5(b) reveals that the impact of uplink NR-U interference on uplink Wi-Fi performance is the same when $\beta_{WN} = -82$dBm for the SU mode and $\beta_{WN} = -72$dBm for the MU OFDMA mode. *Although these discussions have been presented through Fig. 5 for a specific set of parameters, we verify that they are also true for other choices of $M_Y^T, Q_Y^{sch}, \epsilon_Y$, and β_{YZ}.*

Summary: We conclude that for a given number of potential interferers, NR-U performance in the presence of potential uplink Wi-Fi interference is strictly better when Wi-Fi STAs use the MU OFDMA mode instead of the SU mode. At the same time, the uplink performance in Wi-Fi is also significantly better when Wi-Fi uses the MU OFDMA mode and schedules more than one STAs at a time. The benefits for NR-U arise from the added sensing requirement at the AP when MU OFDMA-based uplink transmissions are scheduled, while those for Wi-Fi arise from reduced hidden node probability due to more than one simultaneous transmitters.

D. Importance of accurate sensing at the AP/gNB

1) Impact of number of scheduled uplink transmitters: Fig. 6(a) shows the impact of the number of scheduled uplink transmitters on the success probability of RAT Y. In Fig. 6(a), Y is Wi-Fi while the interfering RAT Z is NR-U. Observe that as the number of scheduled transmitters increases, the success probability of each of these transmissions increases. This can be understood intuitively as follows: as the number of active Wi-Fi STAs increases, the probability that *at least one* of them is within the sensing range of NR-U devices increases, thereby reducing the hidden node probability, p_H^{WN}. Now consider a scenario where there are ongoing NR-U transmission(s) but the AP falsely infers the channel to be idle and schedules uplink users. Such a scenario can arise if the AP is hidden to the ongoing NR-U transmission(s). Fig. 6(b) shows the success probability of downlink NR-U transmissions in the presence of uplink MU OFDMA Wi-Fi interferers. Observe that as the hidden AP schedules more number of uplink STAs, the resulting impact on downlink NR-U worsens.

2) Impact of transmit power control: Fig. 6(c) shows the impact of transmit power control used in uplink MU OFDMA Wi-Fi transmissions in the presence of downlink NR-U interference. We observe that as far as the success probability of Wi-Fi is concerned, higher the value of ϵ_W used by the STAs, the more probable is the successful reception of these packets at the AP. This follows from observing Eq. (4). A higher value of ϵ_W provides more compensation for the path loss encountered in transmitting a signal. This leads to high transmission powers at STAs located far from the AP, which diminishes the probability of these STAs being hidden to other devices. On the other hand, if the Wi-Fi AP has falsely concluded that the channel is idle, when, in fact, there are ongoing NR-U transmissions, a higher ϵ_W has the opposite effect on NR-U transmissions. This is shown in Fig. 6(b), which shows the impact of uplink Wi-Fi interference on downlink NR-U
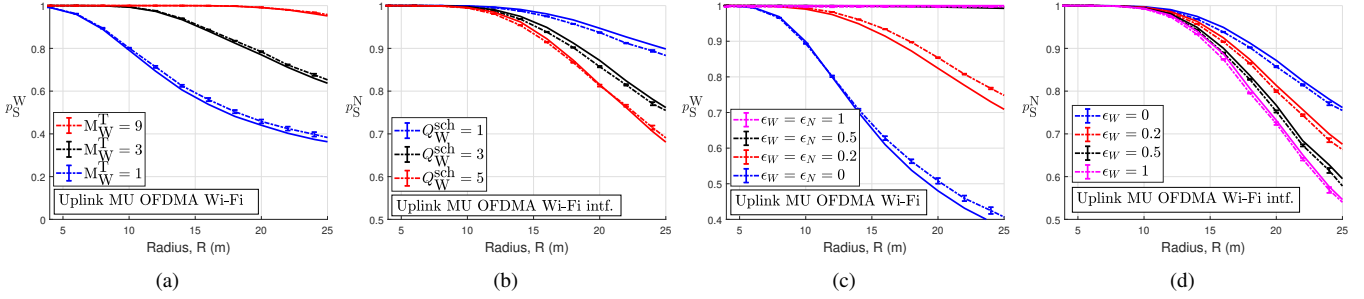
Fig. 6: (a) Impact of number of scheduled RAT Y (Wi-Fi) transmitters, downlink NR-U intf., $\epsilon_W=0$ (b) Impact of number of scheduled RAT Z (Wi-Fi) interferers on downlink NR-U, (c) Impact of power control at RAT Y (Wi-Fi), $M_W^T=3$, downlink NR-U intf., (d) Impact of power control at RAT Z (Wi-Fi) on downlink NR-U, $Q_W^{sch}=3$.
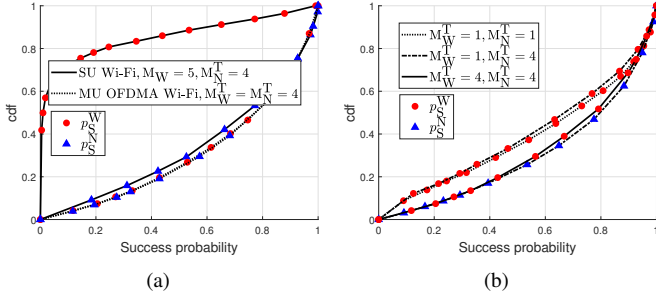

Fig. 7: Simulation results for three co-channel Wi-Fi and NR-U networks, $\epsilon_W=\epsilon_N=0.2$, (a) legacy contention (SU) vs MU OFDMA for uplink Wi-Fi, (b) impact of number of scheduled transmitters.

transmissions. Note that all the aforementioned discussions on Fig. 6 also apply to uplink NR-U transmissions.

Summary: We conclude that both factors: (i) a higher number of scheduled users, and (ii) transmit power control, are beneficial in increasing the success probability of uplink transmissions. However, if the channel is busy, and the AP/gNB falsely concludes that the channel is idle, both of these factors exacerbate the interference at the other RAT's receiver.

E. Coexistence of Multiple Wi-Fi and NR-U Networks

In the simulation results discussed next, we randomly place three Wi-Fi APs and NR-U gNBs each in a square region of length 100 m. We place 15 Wi-Fi STAs and 15 NR-U UEs randomly in this region. Each STA/UE is associated with its nearest AP/gNB. All nodes detect each other using a detection threshold of -72 dBm, i.e., $\beta_{WW}=\beta_{WN}=\beta_{NW}=\beta_{NN}=-72$ dBm.

Fig. 7(a) shows the cdf of the success probabilities observed by the Wi-Fi STAs and NR-U UEs under different conditions. The success probability observed at a device is zero if none of its transmitted packets are successfully decoded at the receiver during the simulation interval. First, observe that the success probability of Wi-Fi STAs dramatically improves when they switch from the legacy contention mode to the MU OFDMA mode. Furthermore, as discussed in Sec. VI-C, we observe that this switch also increases the success probability of NR-U UEs, albeit by a modest amount. Next, Fig. 7(b) shows the cdf of Wi-Fi STAs and NR-U UEs under a different number of scheduled transmitters. In all cases reported in Fig. 7(b) Wi-Fi STAs transmit using MU OFDMA. Observe

that when the number of scheduled transmitters are equal for both RATs, an increase in M_Y^T (from 1 to 4) increases the success probability of both RAT's transmissions[7]. On the other hand, if one of the RATs schedules more users than the other (NR-U in Fig. 7(b)), we observe that the success probability of that RAT's transmissions (i.e., NR-U) increases while that of the other RAT (i.e., Wi-Fi) drops by a small amount. Thus, scheduling more uplink transmitters results in an increase in the success probability of their transmissions. We observe the same phenomenon with transmit power control (as discussed in Sec. VI-D2). We omit these results in the interest of space.

We note that the above results differ from those discussed in the preceding subsections. Results in Fig. 7 also account for packet losses due to the simultaneous countdown of the backoff counter to zero, whereas we ignore these in our analysis. Nevertheless, the above discussions highlight that *although our analysis was derived for the case of only one co-channel Wi-Fi and NR-U networks, the insights derived from the model also apply when more than one Wi-Fi and NR-U networks coexist.*

VII. Conclusions & Future Work

In this paper, using a stochastic geometry-based model and extensive simulations, we investigate the factors that critically affect the success probability of Wi-Fi 6E and NR-U transmissions when the two technologies coexist in the 6 GHz bands. We identify that compared to CSMA/CA, schedule-based uplink MU OFDMA transmissions improve the success probability of NR-U transmissions as well as those of Wi-Fi 6E uplink. This is a critical finding for the 6 GHz bands, where there are no current Wi-Fi or 3GPP-based unlicensed technologies in operation. Consequently, CSMA/CA for uplink access can indeed be disabled in these bands.

We limit our work in this paper to the success probability of individual transmissions. Although this has implications on user-perceived system-level metrics like the throughput and the latency, other factors can come into play in LBT-based networks. For example, we ignore the exposed node problem in our work, which, in many cases, is known to contribute negatively to the overall system performance. We leave the extension of our work to include a study on the exposed node problem and system-level metrics to future work.

---

[7]In the MU OFDMA mode, when $M_W^T=M_N^T$, $p_S^W=p_S^N$ (see Fig. 7(a) for $M_W^T=M_N^T=4$). Hence, for cases where $M_W^T=M_N^T$, we only show p_S^W in Fig. 7(b).

REFERENCES

[1] FCC, "Report and Order and Further Notice of Proposed Rule-making; In the Matter of Unlicensed Use of the 6 GHz band (ET Docket No. 18-295); Expanding Flexible Use in Mid-Band Spectrum Between 3.7 and 24 GHz (GN Docket No. 17-183)." https://docs.fcc.gov/public/attachments/FCC-20-51A1.pdf, April 2020.

[2] European Commission, "Mandate to CEPT to study feasibility and identify harmonized technical conditions for wireless access systems including radio local area networks in the 5925-6425 MHz band for the provision of wireless broadband services," December 2017.

[3] G. Naik, J. Liu, and J.-M. J. Park, "Coexistence of wireless technologies in the 5 ghz bands: A survey of existing solutions and a roadmap for future research," *IEEE Communications Surveys & Tutorials*, vol. 20, no. 3, pp. 1777–1798, 2018.

[4] IEEE, "IEEE P802.11ax/D6.1; Part 11: Wireless LAN Medium Access Control (MAC) and Physical Layer (PHY) Specifications; Amendment 1: Enhancements for High Efficiency WLAN," May 2020.

[5] D. López-Pérez, A. Garcia-Rodriguez, L. Galati-Giordano, M. Kasslin, and K. Doppler, "IEEE 802.11 be Extremely High Throughput: The Next Generation of Wi-Fi Technology Beyond 802.11 ax," *IEEE Communications Magazine*, vol. 57, no. 9, pp. 113–119, 2019.

[6] E. Khorov, I. Levitsky, and I. F. Akyildiz, "Current Status and Directions of IEEE 802.11be, the Future Wi-Fi 7," *IEEE Access*, pp. 1–1, 2020.

[7] 3GPP, "3GPP TS 37.213: Physical layer procedures for shared spectrum channel access (Release 16) ," July 2020.

[8] 3GPP, "3GPP TR 38.889: Technical Specification Group Radio Access Network; Study on NR-based access to unlicensed spectrum (Release 16) ," Dec. 2018.

[9] S. Lagen, L. Giupponi, S. Goyal, N. Patriciello, B. Bojovic, A. Demir, and M. Beluri, "New Radio Beam-based Access to Unlicensed Spectrum: Design Challenges and Solutions," *IEEE Communications Surveys & Tutorials*, 2019.

[10] S. Falahati, G. Hiertz, and N. Madhavan, "IEEE 802.11-19/1083r1: Coexistence in 6 GHz License-exempt Spectrum." presented at the P802.11 Coexistence SC workshop, July 2019.

[11] B. Chen, J. Chen, Y. Gao, and J. Zhang, "Coexistence of LTE-LAA and Wi-Fi on 5 GHz with corresponding deployment scenarios: A survey," *IEEE Communications Surveys & Tutorials*, vol. 19, no. 1, pp. 7–32, 2016.

[12] G. Naik, J.-M. Park, J. Ashdown, and W. Lehr, "Next generation Wi-Fi and 5G NR-U in the 6 GHz bands: Opportunities and challenges," *IEEE Access*, vol. 8, pp. 153027–153056, 2020.

[13] Y. Li, F. Baccelli, J. G. Andrews, T. D. Novlan, and J. C. Zhang, "Modeling and analyzing the coexistence of Wi-Fi and LTE in unlicensed spectrum," *IEEE Transactions on Wireless Communications*, vol. 15, no. 9, pp. 6310–6326, 2016.

[14] A.-k. Ajami and H. Artail, "On the modeling and analysis of uplink and downlink IEEE 802.11 ax Wi-Fi with LTE in unlicensed spectrum," *IEEE Transactions on Wireless Communications*, vol. 16, no. 9, pp. 5779–5795, 2017.

[15] A. Mbengue and Y. Chang, "Performance analysis of LAA/Wi-Fi coexistence: Stochastic geometry model," in *2018 IEEE Wireless Communications and Networking Conference (WCNC)*, pp. 1–6, IEEE, 2018.

[16] X. Wang, T. Q. Quek, M. Sheng, and J. Li, "Throughput and fairness analysis of Wi-Fi and LTE-U in unlicensed band," *IEEE Journal on Selected Areas in Communications*, vol. 35, no. 1, pp. 63–78, 2016.

[17] A. Bhorkar, C. Ibars, and P. Zong, "On the throughput analysis of LTE and WiFi in unlicensed band," in *2014 48th Asilomar Conference on Signals, Systems and Computers*, pp. 1309–1313, IEEE, 2014.

[18] B. Bellalta, "IEEE 802.11 ax: High-efficiency WLANs," *IEEE Wireless Communications*, vol. 23, no. 1, pp. 38–46, 2016.

[19] M. Burton and G. Hill, "802.11 Arbitration," *White Paper, Certified Wireless Network Professional Inc., Durham, NC*, 2009.

[20] G. Alfano, M. Garetto, and E. Leonardi, "New insights into the stochastic geometry analysis of dense CSMA networks," in *2011 Proceedings IEEE INFOCOM*, pp. 2642–2650, IEEE, 2011.

[21] M. Mehrnoush, V. Sathya, S. Roy, and M. Ghosh, "Analytical modeling of Wi-Fi and LTE-LAA coexistence: Throughput and impact of energy detection threshold," *IEEE/ACM Transactions on Networking (TON)*, vol. 26, no. 4, pp. 1990–2003, 2018.

[22] R. K. Ganti and M. Haenggi, "Spatial and temporal correlation of the interference in ALOHA ad hoc networks," *IEEE Communications Letters*, vol. 13, no. 9, pp. 631–633, 2009.

[23] Z. Gong and M. Haenggi, "Interference and outage in mobile random networks: Expectation, distribution, and correlation," *IEEE Transactions on Mobile Computing*, vol. 13, no. 2, pp. 337–349, 2012.

[24] J. Guo, S. Durrani, and X. Zhou, "Outage probability in arbitrarily-shaped finite wireless networks," *IEEE Transactions on Communications*, vol. 62, no. 2, pp. 699–712, 2014.

[25] J. G. Andrews, A. K. Gupta, and H. S. Dhillon, "A primer on cellular network analysis using stochastic geometry," *arXiv preprint arXiv:1604.03183*, 2016.

[26] J. Meinilä, P. Kyösti, *et al.*, "D5. 3: WINNER+ final channel models," *Wireless World Initiative New Radio WINNER*, 2010.

[27] Cisco, "Enterprise Best Practices for iOS devices and Mac computers on Cisco Wireless LAN," *White Paper*, January 2018.

[28] K. Kim, L. Li, E. Perahia, D. Stanley, S. Strickland, and C. Vlachou, "LAA/Wi-Fi Coexistence Evaluations With Commercial Hardware." presented at the P802.11 Coexistence SC workshop, July 2019.

[29] Cisco Systems Belgium, "BRAN(19)103023: Response to BRAN(19)103016." presented at ETSI BRAN # 103, October 2019.